Published in final edited form as:
J Immunol. 2011 July 1; 187(1): 212–221. doi:10.4049/jimmunol.1002328.

Aborted Germinal Center Reactions and B Cell Memory by Follicular T Cells Specific for a B Cell Receptor V Region Peptide

Ryan A. Heiser, **Christopher M. Snyder**[1], **James St. Clair**, and **Lawrence J. Wysocki**
Integrated Department of Immunology, National Jewish Health and University of Colorado Denver, School of Medicine, Denver, CO 80206

Abstract

A fundamental problem in immunoregulation is how $CD4^+$ T cells react to immunogenic peptides derived from the V region of the BCR that are created by somatic mechanisms, presented in MHC II, and amplified to abundance by B cell clonal expansion during immunity. BCR neo Ags open a potentially dangerous avenue of T cell help in violation of the principle of linked Ag recognition. To analyze this issue, we developed a murine adoptive transfer model using paired donor B cells and CD4 T cells specific for a BCR-derived peptide. BCR peptide-specific T cells aborted ongoing germinal center reactions and impeded the secondary immune response. Instead, they induced the B cells to differentiate into short-lived extrafollicular plasmablasts that secreted modest quantities of Ig. These results uncover an immunoregulatory process that restricts the memory pathway to B cells that communicate with CD4 T cells via exogenous foreign Ag.

During primary humoral immune responses, Ag-reactive B cells undergo developmental and selection processes within germinal centers (GC) that change the isotype of the BCR and improve its avidity for immunogen via class switch recombination and somatic hypermutation (SHM), respectively. As a consequence of diversity within responding clones and subsequent SHM, myriad activated B cells compete for immunogen to receive activating signals directly via BCR aggregation and indirectly via T cell help specified by MHC II-presented peptides derived from the immunogen. This competition provides at least some of the selection pressure for the evolution of high-affinity memory B cell clones that persist and protect against secondary challenge (1–5).

Robust GC reactions and SHM require a cognate Ag-specific interaction between T and B cells, during which signals in the form of membrane contacts and cytokines provide vital help to B cells. This help is delivered by specialized T follicular helper cells (T_{FH}), recently described phenotypically as $CD4^+$ $CXCR5^+$ and $ICOS^{high}$ (6–10). Whereas SHM produces the extensive BCR diversity required for affinity maturation during GC reactions, it can also generate autoreactive BCR (11). A requirement for T_{FH} cell help during the GC response most likely acts as a safeguard to prevent B cells that acquire self-specificity via SHM from participating in an autoimmune response because T_{FH} cell help to autoreactive B cells should be absent or severely limited due to self-tolerance. If T_{FH} cells were not tolerant of BCR V region peptides, however, they could potentially help GC B cells via cognate

Address correspondence and reprint requests to Prof. Lawrence J. Wysocki, Department of Immunology, K902, National Jewish Health, 1400 Jackson Street, Denver, CO 80206. WysockiL@NJHealth.org.
[1]Current address: Department of Microbiology and Immunology, Jefferson University, Philadelphia, PA.

The online version of this article contains supplemental material.

Disclosures
The authors have no financial conflicts of interest

interactions directed by these peptides because activated B cells proficiently self-present BCR-derived peptides in MHC II (12–16). We refer to this as the receptor presentation avenue of help (17). The potential danger posed by receptor presentation is illustrated by the development of autoimmunity in two experimental models involving transgenic T cells specific for BCR peptides (18, 19). Studies in spontaneously autoimmune humans and nontransgenic mice suggest that this avenue of help may be active in disease settings (17, 20–22).

$CD4^+$ T cells attain a state of self-tolerance to germline-encoded peptides derived from Ig V regions (23, 24). In contrast, peptides encoded by somatically diversified sequences generated at junctional boundaries by V/D/J recombination or throughout the V region by SHM can be immunogenic (25–27). As such, activated B cells are poised to receive help from T_{FH} cells via the receptor presentation avenue. Due to the enormous number of unique BCR-derived peptides arising in the GC, it is likely that T_{FH} cells encounter antigenic BCR V region peptides on a regular basis. For this reason, it is important to understand the consequences of these interactions with respect to immunoregulation.

To investigate the outcome of a direct interaction between a T cell and a GC B cell that occurs via receptor presentation under physiological circumstances, we established an adoptive transfer model with donor B and T cells from complementary Igκ and αβTCR transgenic mice. We demonstrate that a cognate BCR peptide-directed interaction between B and T cells disrupts GC B cell development and inhibits B cell memory responses in favor of short-lived plasmablast differentiation.

Materials and Methods

Mice

CA30 αβTCR and Igκ36-71 (κTg) transgenes have been described (16, 18). They were bred onto an A/J genetic background through >10 and >20 backcross generations, respectively. A targeted κ deficiency (28) was bred onto the A/J genetic background for 10 generations. CA30 $\kappa^{-/-}$ and κTg $\kappa^{-/-}$ mice were bred from these strains and used in all of the experiments. For adoptive transfers taken to day 135, 4-mo-old $\kappa^{-/-}$ offspring from $\kappa Tg^{+/-}$ $\kappa^{-/-}$ mothers were used as recipients.

Adoptive transfers, immunizations, and injections

On day 0 of the standard adoptive transfer, 8- to 16-wk-old nonirradiated A/J $\kappa^{-/-}$ mice were injected i.v. with enriched B cells or unfractionated splenocytes taken from κTg $\kappa^{-/-}$ mice. At 4 h posttransfer, mice were immunized i.p. with 100 μg goat anti-mouse Ig-κ (GαMκ; Bethyl Laboratories, Montgomery, TX) precipitated in alum. GαMκ was precipitated with $AlKSO_4$ and $NaHCO_3$ and washed three times in PBS before injection. On day 7, experimental animals received 2.5×10^5 unfractionated CA30 $\kappa^{-/-}$ lymph node (LN) cells i.v., unless otherwise indicated. In some experiments, enriched CA30 T cells were labeled with CFSE (Molecular Probes, Eugene, OR), as previously described (29). Recipient mice were sacrificed on day 10, 12, 14, or 137. For memory experiments, booster immunizations were given i.p. on day 135 with 50 μg GαMκ in sterile PBS.

Variations of the standard adoptive transfer are indicated in *Results*. For experiments shown in Fig. 6, GαMκ was conjugated with the VκFR1 peptide (DIQMTQIPSSLSASLGDRVSISC) or control peptide (CtrlP) (CARAVGTTRARGAWFA) through the peptide cysteines using sulfosuccinimidyl-4-[*N*-maleimidomethyl]cyclohexane-1-carboxylate (Pierce, Rockford, IL), according to the manufacturer's protocol. Prior to their use as immunogens in vivo, VκFR1-GαMκ and CtrlP-

GαMκ were tested on A/J B cells for their ability to acquire VκFR1-GαMκ through the BCR and to stimulate VκFR1-specific naive CA30 T cells (Supplemental Fig. 4).

Flow cytometry

Splenocytes or LN cells were isolated from recipient animals by gently pressing spleens and LN though a BD Falcon 70-mm nylon cell strainer (BD Bioscience, Bedford, MA) using a syringe plunger. Erythrocytes were lysed with RBC lysis buffer (Sigma-Aldrich). Cells were stained in PBS with 2% FCS at 4°C for 30 min. In stains involving both anti-mouse κ and mAb17-63, cells were incubated first with biotin-mAb17-63, washed, and then stained with rat anti-mouse κ. Anti-CD45R/B220 (clone RA3-6B2), anti–PD-1 (clone RMP1-30), anti-ICOS (clone C398.4A), and anti-CD4 (clone IM7) were purchased from Biolegend (San Diego, CA). Anti-κ (clone 187.1) and anti-CXCR5 were purchased from BD Biosciences (San Jose, CA). Anti-CD4 (clone GK1.5) was purchased from eBioscience (San Diego, CA). mAb17-63 (mouse κ, IgG2b) was generated in house and biotinylated using EZ-link NHS-LC-biotin from Thermo Scientific (Rock-ford, IL). Streptavidin–allophycocyanin/Cy7 from Biolegend was paired with biotinylated mAb17-63. VκFR1 tetramer was made in house, as previously described (18). Samples were analyzed on either FACSCalibur or FACScan flow cytometers (BD Biosciences, San Jose, CA) using FlowJo (Tree Star, San Carlos, CA) software.

Immunohistology of frozen sections

The 6-μm sections of frozen spleen or LN embedded in Tissue-Tek OCT compound (Sakura Finetek USA, Torrence, CA) were fixed in acetone, dried, and kept at −70°C. Sections were rehydrated in PBS and incubated in blocking buffer (PBS, 4% normal rat serum, 0.1% sodium azide) at room temperature (20 min) in a humidified chamber. Sections were stained with mAb in blocking buffer (20 min) and washed by PBS immersion (2 min). Slides were stained simultaneously with master mix cocktails of rat anti-mouse κ (clone 187.1) peanut agglutinin (PNA; Vector Laboratories, Burlingame, CA) and anti-mouse B220 (clone RA3-6B2-allophycocyanin; Biolegend) in PBS with 2% FCS. Other stains included anti-mouse CD11c (clone N418) and anti-mouse Vβ8.1, 8.2 TCR (clone KJ16) (eBioscience). Streptavidin-Cy3 (Sigma-Aldrich) was used as a secondary reagent for all biotinylated Abs. For amplification of CFSE signal, DyLight 488 anti-FITC (Jackson ImmunoResearch Laboratories, West Grove, PA) was used. Stained slides were mounted with Biomeda Gel/Mount (Fisher Scientific, Pittsburgh, PA) and viewed with an inverted Zeiss 200M confocal microscope at 25°C. Images were collected with Slidebook software (Intelligent Imaging Innovations, Denver, CO).

In the BrdU incorporation experiment, mice were injected with 1 mg BrdU in PBS, i.p., 4 h prior to sacrifice. Spleens were frozen in OCT media and 6-μm sections were fixed in 4% paraformaldehyde for 30 min at 4°C. Slides were washed 5 min in PBS with 1% Triton X-100 (PBS/Triton) three times. Washed slides were submerged in 1 N HCl for 10 min, followed by 30 min in 2 N HCl at 37°C. Following acid washes, slides were submerged in 0.1 M borate buffer for 10 min at room temperature. Slides were washed as before in PBS/Triton. Tissue sections were incubated in blocking solution (PBS/Triton, 5% FCS) for 1 h. Anti-BrdU FITC Ab (BD Biosciences) was applied overnight in blocking buffer. The next day, slides were washed in PBS/Triton three times and mounted with Biomeda Gel/Mount (Fisher Scientific).

Quantification of serum κTg Ab and total κ Ab

Microlon ELISA plates (Greiner Bio-One, Monroe, NC) were coated with mAb17-63 and rat γ-globulin (each at 2.5 μg/ml) in PBS overnight at 4°C and then incubated in blocking buffer (PBS, 2% BSA, 1% gelatin, 0.05% Tween 20) for 2 h at 37°C. Serial 2-fold dilutions

of test sera were added to wells. An equal volume of the ligand, biotinylated mAb36-71 (IgG1), was added to every well (250 ng/ml) and plates were incubated at 4°C for 4 h. Plates were washed with PBS, and Delfia SA-europium (Wallac, Turku, Finland) was applied. Following 2-h incubation at 4°C, plates were washed with PBS and developed in europium enhancement solution (100 mM sodium acetate, 1 mM thenoyltrifluoroacetone, 750 mM tri-octylphosphineoxide [pH 3.2]) made in house. Europium counts were read in a Wallac Victor 2 plate reader at 590 nm, for 1 s/well. Purified unlabeled mAb36-71 was used to generate a standard competition curve. Calculations were done using Prism graphing software (GraphPad Software, La Jolla, CA). Serum κ Ab quantification was performed following the same general competition ELISA, using a rat anti-mouse κ L chain (clone 187.1) to coat plates. The anti-goat IgG ELISA was performed by coating Microlon ELISA plates with goat IgG (Sigma-Aldrich). Serial 2-fold dilutions of test sera were added to coated wells. Goat anti-mouse IgG HRP (Southern Biotechnology Associates, Birmingham, AL) was used to detect bound mouse IgG. The specificity of mAb17-63 was tested by ELISA in plates coated with 2 μg/ml mAb17-63 (IgG2b, κ). Selected κ^+ IgM^+ Abs were added to the plates in serial 2-fold dilution, starting at 2 μg/ml. Plates were developed with a HRP-labeled anti-mouse IgM (Southern Biotechnology Associates).

ELISPOT assay

Microlon ELISA plates were coated with either 5 μg/ml polyclonal goat anti-mouse IgG1, goat anti-mouse IgM, or 1 μg/ml purified protein L (Pierce, Rockford, IL) in PBS overnight at 4°C. Plates were blocked with RPMI 1640 with 10% FCS for 2 h at 37°C. Splenocytes (5.0×10^5) were added to the first well of a row and titrated in serial 2-fold dilution in RPMI 1640 with 10% FCS. After 7 h, plates were washed three times with PBS and 0.05% Triton X-100. Biotinylated mAb17-63 (IgG2b) or HRP-coupled goat anti-mouse IgG1 or IgM (Southern Biotechnology Associates) was applied at 0.5 ng/ml in blocking buffer and allowed to incubate overnight at 4°C. Plates were washed in PBS, and streptavidin-alkaline phosphatase (Biolegend) was applied at 1:2000 in blocking buffer. After washing, plates were developed in 100 mM Tris-HCl (pH 9.5), 100 mM NaCl, and 10 mM $MgCl_2$ with 1 mg/ml 5-bromo-4-chloro-3-indolyl phosphate (Pierce) for 2 h at 37°C. Plates were scanned into TIFF images for blinded counting.

Results

$CD4^+$ T cells specific for a BCR-derived peptide disrupt B cell participation in the GC reaction

To determine the consequences of a cognate interaction between GC B cells and BCR peptide-specific T cells, we used a specialized pair of transgenic mice in an adoptive transfer protocol. One mouse (κTg) expresses a κ L chain transgene derived from the 36-71 hybridoma (30). This hybridoma was originally generated during an antihapten immune response and expresses a Vκ gene carrying a pair of somatic mutations in the region encoding framework 1 that generate an immunogenic $I\text{-}A^k$–restricted peptide, referred to in this study as the VκFR1 peptide (26). κTg B cells express endogenous H chains, resulting in a diverse repertoire within the κTg B cell population, much of which is in a resting state (16). Another mouse, CA30, expresses a transgenic αβ TCR able to engage the VκFR1 peptide in the context of $I\text{-}A^k$ (18). Most of the CA30 T cells are Ag inexperienced, as assessed by the low frequency of those that are $CD44^{high}$ (~2%).

In the standard adoptive transfer experiment, 5.0×10^4 κTg $\kappa^{-/-}$ splenocytes, or an equivalent number of purified κTg $\kappa^{-/-}$ B cells, were injected into mice deficient for the Ig κ L chain ($\kappa^{-/-}$) (Fig. 1*A*). Using $\kappa^{-/-}$ recipient mice (28) allowed us to specifically stimulate transferred B cells, track their developmental progress, and assess κ^+ Ab production. To

recruit these cells into an immune response, recipients were immunized i.p. with a goat anti-mouse Igκ polyclonal Ab (GαMκ) precipitated in alum. The goat Ab specifically aggregates the BCR of transferred B cells, and elicits endogenous $CD4^+$ T cells that are specific for goat Ig and that provide the necessary help for GC development (31). Without GαMκ immunization, GC are not induced. On day 7, during GC formation, 2.5×10^5 CA30 $\kappa^{-/-}$ whole LN cells or an equivalent number of purified CA30 $\kappa^{-/-}$ T cells were transferred into experimental recipients. We used this protocol to model a scenario in which $CD4^+$ T cells interact with GC B cells via somatically generated BCR-derived peptides. Specifically, we wanted to determine whether such an interaction promoted a normal B cell response as seen with conventional immunogens, or whether B cell differentiation and memory development were prohibited or altered in some way.

Seven days after transfer of κTg cells and immunization, κ^+ PNA^+ GC were found in spleen, as assessed by immunofluorescent staining of frozen sections (Fig. 1*B*). At day 10, immunofluorescent staining of frozen spleen sections showed that in recipients of κTg cells alone, κ^+ cells were tightly localized within PNA^+ GC areas (Fig. 1*C*, *top left*). In contrast, mice that received CA30 T cells 3 d before had fewer κ^+ cells located in GC, with many distributed in outer follicular and T cell areas (Fig. 1*C*, *bottom left*). The follicular distribution of κ^+ cells observed in spleens of mice receiving CA30 T cells suggests an ongoing exodus of κ^+ B cells out of the GC. Notably, this distribution is very similar to that seen by Fooksman et al. (32) in their study of GC B cell differentiation. Nevertheless, additional studies will be required to test this interpretation conclusively.

In this adoptive transfer system, peak GC responses in the spleen were seen on day 14. At this time, recipients of κTg cells alone had many large GC with some plasma cells scattered throughout the red pulp (Fig. 1*C*, *top right*). In recipients of CA30 T cells, in contrast, there was a striking redistribution of brightly staining κ^+ B cells to the red pulp, splenic vasculature, and bridging channels adjacent to T cell areas, with few κ^+ cells localized in GC (Fig. 1*C*, *bottom right*). κ^+ cells remaining near the GC were found almost exclusively at the T–B border (Fig. 1*C*, *bottom right*). Coadoptive transfers of κTg cells and CA30 cells on day 0 produced similar results by day 14 (Supplemental Fig. 1*A*). In addition, a similar redistribution and expansion of κ^+ B cells were evident in paracortical and medullary regions of LN (Supplemental Fig. 1*B*). Finally, loss of κTg B cells from the GC in mice receiving CA30 T cells was also observed when we used protein L in place of GαMκ as a polyclonal Ag to selectively activate κ^+ B cells (Supplemental Fig. 1*C*).

BCR peptide-specific T cells enter the GC

To determine whether transferred CA30 T cells entered ongoing GC reactions containing κTg B cells, purified CFSE-labeled CA30 T cells were injected into recipients on day 7 following transfer of κTg cells on day 0. Control A/J recipients of CA30 T cells were immunized with the VκFR1 peptide. Spleens were collected at 50 h and examined by immunofluorescence. Although CA30 T cells had lost most of their green fluorescence due to cell division, they could be detected with a DyLight-488–labeled anti-FITC mAb (Fig. 2*A*). This enhancement revealed multiple individual CA30 T cells, as well as clusters of CA30 T cells, in GC of mice that received κTg cells. Additional stains with anti-CD4 and anti-Vβ8.1/8.2 (the β-chain expressed by CA30 T cells) verified the identity of these cells (Fig. 2*B*). In peptide-immunized mice or unimmunized control mice, CFSE-labeled CA30 T cells were found exclusively in T cell areas (Fig. 2*A*, *middle*, *right*). By day 14, unambiguous identification of CFSE-labeled CA30 T cells was no longer possible; however, numerous cognate interactions between $V\beta8.1/8.2^+$ cells and remaining κ^+ cells were found within GC (Fig. 2*C*).

In this transfer system, CA30 T cells can be distinguished from host T cells by flow cytometry with the tetrameric staining reagent, I-A^k-VκFR1 (18). To determine whether CA30 T cells became activated during immune responses by κTg B cells, we analyzed CA30 T cells recovered at day 10 from standard adoptive recipients. A positive control group of A/J mice received CA30 cells and was immunized with the VκFR1 peptide. By 3 d after transfer, tetramer-positive T cells in both groups had upregulated ICOS, CD44, CXCR5, and PD-1 (Fig. 2*D*). CA30 T cells of the experimental group consistently stained brighter for ICOS and with the I-A^k-VκFR1 tetramer than those of the peptide-immunized positive control group (Fig. 2*D*). Elevated expression of ICOS and CXCR5 was indicative of a T follicular phenotype and in agreement with the presence of conjugates between CA30 T cells and κTg B cells in the GC. Collectively, the data indicated that GC dissolution was most likely due to CA30 T cells that had entered the GC.

BCR peptide-specific T cells drive development of plasmablasts in the red pulp and T cell zones

The preceding immunofluorescence analyses of spleen sections revealed that by 3 d following adoptive transfer of CA30 T cells, κTg B cell participation in GC reactions was severely disrupted. At this time, many κ^+ cells were found throughout follicles, T cell areas, and bridging channels between the GC and the red pulp, consistent with an exodus of κTg B cells from the GC. The extrafollicular aggregates of κ^+ B cells in spleens and LN were largely $IgG1^+$, as were the κ^+ B cells found in GC of control animals (data not shown). This phenotype was exaggerated by day 14 (7 d after CA30 T cell transfer), at which time large extra-follicular aggregates of κ^+ cells were evident in the red pulp and often adjacent to T cell areas. Their relatively bright κ staining, large numbers, and location at bridging channels suggested that these cells were plasmablasts. In agreement with this, the κ^+ extrafollicular cells did not express as much B220 as other cells within the grouping (Fig. 3*A*). Furthermore, a portion of these cells was dividing within extrafollicular clusters during a brief 4-h pulse with BrdU prior to harvest (Fig. 3*A*). Within these κ^+ clusters, other unidentified cells also appeared to be proliferating. In addition, the κ^+ aggregates tightly colocalized with a $CD11c^+$ population in the splenic red pulp of mice that received CA30 T cells (Fig. 3*B*). Plasmablast clusters in the red pulp during an immune response to NP-Ficoll have been reported to be in close association with $CD11c^+$ dendritic cells in mice that also received anti-CD40 (33).

If the large clusters of κ^+ B cells observed in our adoptive transfer were plasmablasts, there should be more Ab-secreting cells (ASC) in recipients of CA30 T cells. ELISPOT assays revealed that there was a 35-fold increase in κ^+ $IgG1^+$ ASC, and a 7.5-fold increase in κ^+ IgM^+ ASC in recipients of CA30 cells relative to controls at day 14 (Fig. 3*C*). In agreement with this result, the concentration of serum κ^+ Ab was significantly increased in recipients of CA30 T cells at day 14 (Fig. 3*D*). However, it was not increased proportionally to the increase in ASC numbers. This quantitative discordance between increased κ^+ ASC numbers and serum κ^+ Ab is also consistent with the interpretation that the ASC in CA30 recipients were plasmablasts, whereas the ASC in the κTg-only recipients were comprised mostly of fully differentiated plasma cells. Notably, the κ^+ ASC from recipients of CA30 T cells produced smaller spots in the assay than ASC from control mice that received only κTg cells (Fig. 3*E*).

T cells specific for a BCR-derived peptide engage in cognate interactions with GC B cells

It was possible that GC disruption was the consequence of a nonspecific effector mechanism, perhaps mediated by a cytokine or through disruption of follicular dendritic cells. To address this, we performed standard adoptive transfers with mixed populations (1:1) of purified κTg and normal (A/J) B cells. κTg B cells can be reliably discriminated

from A/J B cells by flow cytometry with a mAb (mAb17-63), specific for mutations in the κTg L chain (Supplemental Fig. 2*A*, 2*B*). As before, CA30 T cells were transferred to recipients 7 d after B cell transfer and immunization. Three days following T cell transfer, relative GC occupancy ($B220^+$ PNA^{high}) of κTg and κ^+ A/J B cells was assessed by flow cytometry with anti-κ and mAb17-63. We chose the day 10 time point because it represents a dynamic period between GC participation by κTg B cells and their redistribution to extrafollicular regions in recipients of CA30 T cells.

In mice that did not receive CA30 T cells, κTg B cells comprised an average of 54% of the $B220^+$ PNA^{high} κ^+ population, closely reflecting the initial transfer ratio. In contrast, κTg B cells comprised only 34% of the $B220^+$ PNA^{high} κ^+ population in recipients of CA30 T cells (Fig. 4). The intermediate loss of κTg B cells from the GC at day 10, as assessed by flow cytometry, reflected the comparable loss observed by immunofluorescence in spleen sections at this time (Fig. 1*C*), and was highly significant ($p = 0.0001$; Fig. 4*B*). This result was consistent with the presence of conjugates between CA30 T cells and κTg B cells within the GC. It indicates that the loss of κTg B cells from GC and their differentiation into extrafollicular plasmablasts are the result of a selective cognate interaction between CA30 T cells and κTg B cells.

Inhibition of a memory B cell response by BCR peptide-specific T cells

Because CA30 T cells selectively inhibited the development of GC κTg B cells, we predicted they would similarly inhibit development of κTg memory cells and long-lived plasma cells in the bone marrow, both of which pass through the GC stage. To test this idea, we allowed the standard adoptive transfer to proceed long-term, bleeding the mice periodically. At day 135, the recipients were rechallenged with GαMκ in saline. At this time, there was very little κ^+ Ab (5.8 μg/ml) in mice that received CA30 T cells. In fact, the small amount of κ^+ Ab observed is approximately what would be predicted to remain after 16 wk, starting with the day 14 κ^+ Ab titer and assuming an Ig $t_{1/2}$ of ~2 wk. In contrast, serum κ^+ Ab persisted longer in mice that did not receive CA30 T cells. Moreover, the baseline concentration of serum κ^+ Ab at day 135 in the κTg-only recipient group was ~10 times more than that in the CA30 recipient group (53.4 μg/ml) (Fig. 5*A*), despite a much higher concentration in the CA30 group at early time points. Furthermore, in a repeat experiment, we found that κ^+ ASC in the bone marrow at day 130 were reduced by ~10-fold in mice that received CA30 T cells on day 7 (data not shown).

Consistent with failed memory development in recipients of CA30 T cells, there were few splenic $IgG1^+$ ASC 50 h following a secondary immunization with GαMκ in saline, and the few ASC observed were primarily from one mouse. In contrast, substantial numbers of $IgG1^+$ $17\text{-}63^+$ ASC by ELISPOT were present in spleens of mice that received κTg cells alone (Fig. 5*B*). In these control mice, the frequency of splenic ASC was ~40-fold higher than that in experimental mice that received CA30 T cells. Although these mice were sacrificed only 50 h following the booster injection, we could nonetheless detect a 30% increase in serum κ^+ Ab of control recipients (Fig. 5*C*). In contrast, no increase was seen in recipients of CA30 cells. Importantly, the endogenous IgG^+ anti-goat Ig titers were indistinguishable between groups 50 h after the booster injection, indicating that inhibition of the memory response was specific for κTg B cells and did not apply to the endogenous λ^+ B cell response against the goat Ig (Fig. 5*D*). Moreover, memory inhibition was not due to an anti-Igκ humoral immune response by recipient IgGl-expressing B cells, as we could not detect such a response in either group of adoptive recipients at early or late time points (data not shown). The reduced titers of persistent κ^+ Ab and lack of a κ^+ secondary immune response indicate that the selective disruption of κTg GC B cells by CA30 T cells impeded their development into both long-lived plasma cells and memory B cells.

Few BCR peptide-specific T cells required for inhibition of GC B cells

Recent studies employing adoptive transfers of transgenic T cells have shown that intraclonal competition among transgenic T cells can influence T cell phenotype, particularly when large numbers of cells are transferred (34). Furthermore, there is evidence that excessive stimulation through the CD40 axis can disrupt GC formation (35). However, in other work, adoptive transfer mice receiving large numbers of paired Ag-specific transgenic T cells (2.5×10^6) and B cells (7.5×10^6) showed normal GC development (36). To address caveats related to nonphysiological numbers of transgenic T and B cells, we repeated the adoptive transfer experiment with 10-fold fewer κTg B cells (5000 splenocytes) and 50-fold fewer CA30 T cells (5000 LN cells). We estimated that of 5000 transferred CA30 LN cells (containing ~4000 CA30 T cells), ~2–10% should be expected to seed the peripheral lymphoid organs, resulting in 80–400 CA30 T cells seated in the mouse (34, 37). This is within the range estimated for endogenous T cells in wild-type mice reactive with a given foreign peptide displayed in MHC II (38).

Analysis of day 12 spleen sections showed that κTg B cells had tightly colocalized with PNA^+ GC areas in control mice (Fig. 6*A*, *top*). In contrast, mice that received 5000 CA30 LN cells on day 6 had κTg B cells both within and outside of GC areas, localized to the follicles and T cell area (Fig. 6*A*, *bottom*). Furthermore, there was a significant reduction in the proportion of GC cells that were κ^+ in recipients of CA30 T cells (Fig. 6*B*, 6*C*). Finally, CA30 T cells had expanded and displayed the hallmark high ICOS expression observed in previous transfer experiments (Fig. 6*D*). Together, these results demonstrate that despite transferring relatively few κTg B cells, occupying only a very small proportion of total GC (~7% of total GC B cells at day 12) and a near physiological number of CA30 T cells, we were able to recapitulate the GC morphology and T cell activation state observed in transfer experiments with large cell numbers. This suggests that GC disruption and plasmablast differentiation mediated by T cell interactions with GC B cells presenting BCR-derived peptides may not be due to excessive numbers of Th cells.

Inhibition of GC B cells occurs through the receptor presentation avenue

To further test the idea that the BCR specificity of T cell help, rather than excessive T cell help to exogenous Ag, was respon sible for impaired GC participation and enhanced plasmablast differentiation, we performed an experiment in which OVA-immunized wild-type B6 mice were injected or not with a large number of OT-II cells on day 7. Data of Supplemental Fig. 3 show that neither the GC response nor the anti-OVA Ab response was significantly affected by the transferred OT-II T cells.

Finally, we addressed this question using a different approach in which the VκFR1 peptide was provided to wild-type B cells in the form of an exogenous Ag. This experiment is a better test of the possibility that excess T cell help disrupts GC B cells because the target peptide Ag and the transgenic T cell are the same as those in our standard adoptive transfer model. In this experiment, the VκFR1 peptide was covalently conjugated to GαMκ, and a control conjugate was prepared with an unrelated peptide (CtrlP). A/J splenocytes (5.0×10^4), as a source of κ^+ B cells, were adoptively transferred into κ-deficient recipients that were immunized with either VκFR1-GαMκ or CtrlP-GαMκ in alum. All mice received large numbers of CA30 LN cells (2.5×10^5) on day 7. Because the BCR of A/J B cells does not contain the VκFR1 peptide, this peptide is presented in B cell MHC II following receptor-mediated uptake of exogenous VκFR1-GαMκ, as confirmed by results of a test shown in Supplemental Fig. 4. As in the previous experiment, we saw no evidence of altered B cell differentiation (day 14) by immunofluorescence in recipients injected with VκFR1-GαMκ compared with control recipients injected with CtrlP-GαMκ (data not shown).

A potential caveat in this experiment was that the VκFR1 peptide might have been largely eliminated from the recipients by day 7, when the CA30 T cells were transferred. To provide a more rigorous test, we modified the protocol slightly by immunizing recipients on day 0 with GαMκ, and then injecting VκFR1-GαMκ (50 μg/alum) or the control conjugate at day 7 immediately after the T cell transfer (Fig. 7*A*). It has been shown that Ags injected during the GC phase of an immune response are able to reach GC B cells (39–41). As before, κ^+ B cell participation in the GC response, as assessed by flow cytometry, was not inhibited in recipients injected with VκFR1-GαMκ relative to that of mice injected with CtrlP-GαMκ. Rather, it was modestly, although not significantly, increased (Fig. 7*B*). This is contrary to what was seen in standard adoptive transfer experiments, in which CA30 T cells severely reduced GC occupancy by κTg B cells when measured the same way (Fig. 7*C*). Collectively, these results indicate that a cognate interaction between T follicular cells and B cells leads to a fundamentally different outcome when the interaction is directed by peptides derived from the BCR than when it is directed by peptides derived from exogenous Ag.

Discussion

To investigate the consequences of cognate interactions between CD4 T cells and B cells that are directed by BCR-derived peptides, we designed an adoptive transfer protocol utilizing donor B and T cells from a complementary pair of Igκ and αβTCR transgenic mice. Our experiments uncovered a regulatory process in which the receptor presentation avenue of T–B interaction selectively impedes B cell development in the GC and immunological memory in favor of a short-term plasmablast response. Shortly after transfer, CD4 T cells specific for a BCR-derived epitope were activated and had migrated within ongoing GC. Inhibition of GC maintenance was observed even with few transferred BCR-specific T cells and κTg B cells, and was specific for B cells presenting a BCR-derived peptide, as opposed to bystanders or B cells presenting the same peptide derived from an exogenous immunogen. The impaired GC response was consistent with severely diminished Ab titers at late time points and a missing recall humoral response upon secondary challenge.

To our knowledge, our studies are the first to examine the effects of BCR-specific T cells on an ongoing GC reaction elicited by a T cell-dependent immunogen. The BCR-derived peptide in this model was originally created in the first framework region of a Vκ gene by a pair of somatic mutations that were acquired during an immune response. Upon BCR aggregation or LPS stimulation, this peptide is proficiently displayed by B cells in I-A^k (16, 26). As such, under physiological circumstances, cognate interactions between T follicular cells and B cells that are directed by unique BCR-derived peptides may commonly occur. Because the CD4 T cell repertoire attains a state of tolerance to germline-encoded BCR sequences, these unique peptides would most likely come either from BCR CDR3 sequences or from somatic mutations located throughout the H and L chain V regions (24–26, 27). It is clear from studies of antihapten immune responses that somatic mutations frequently create both autoreactive BCR and MHC II-restricted epitopes for $CD4^+$ T cells (11, 23). Therefore, without some form of censorship, one might expect that BCR peptide-directed T–B collaboration would frequently lead to the development of memory B cells that engage autoantigens and to a chronic state of autoimmunity. Because autoimmunity is the exception and not the rule, we speculated that the receptor presentation avenue of help would be subject to immunoregulation (17).

Controlling access to GC B cells is one form of regulation that could prevent BCR peptide-specific T cells from providing help to GC B cells. In this regard, naive BCR peptide-specific T cells are unlikely to interact with GC B cells. Once activated, however, T cells may gain access to GC B cells due to changes in the expression of chemokine receptors that direct T cell migration (6, 42). As such, for a BCR-specific T cell to interact with a GC B

cell, the T cell presumably must be stimulated by an activated APC beforehand. In principle, a BCR peptide-specific T cell could become activated in one of two ways. It could be activated by an APC that has taken up secreted Ig containing the peptide, or it could be activated by a chance cross-reaction with a foreign immunogen acquired by the APC.

In our model, it is likely that CA30 T cells gain access to the GC by the first of these alternatives, in which they are initially activated by APC that acquire κTg-encoded Ig in the form of immune complexes with GαMκ. This route of activation could also occur in a physiological Ab response, as somatically mutated Ab is secreted within 2 wk of immunization, and the GC response can last for >1 mo (43–45). At first glance, the second scenario, in which a BCR peptide-specific T cell cross-reacts with a peptide from the immunogen, seems improbable. However, although the likelihood that an Ag-reactive αβTCR would cross-react with a particular BCR-derived peptide is very small, SHM-generated diversity among GC B cells is extensive. This can be inferred from the fact that recurrent somatic mutations have been repeatedly observed in V region genes of independent B cell clones from different animals. For example, an identical set of four consecutive somatic mutations in VHCDR2 was reported in three independent B cell lineages responding to the same immunogen in different mice (46). Therefore, SHM may be viewed as a generator of diverse BCR peptide libraries, any one peptide of which may be cross-reactive with respect to a given preactivated T cell. Numerous contacts between T cells and GC B cells would provide ample opportunity for paired interactions between B cells and mutant BCR peptide-specific T cells (47, 48).

In our study, the consequences to the GC B cell of presenting exogenous Ag, versus endogenous BCR-derived Ag, to T cells within the follicle were clear and dramatic: presentation of exogenous Ag promoted GC development, whereas endogenous presentation terminated GC development. Given the abundance of BCR-derived Vκ-FR1 peptide for κTg B cells, it is possible that GC inhibition and plasmablast differentiation were due to an unusually high level of peptide presentation by κTg B cells and the proportional strength of the T–B interaction. Indeed, it has been proposed that high total signal derived from the BCR and/or T cell signals may drive IFN regulatory factor 4 upregulation resulting in plasma cell differentiation (49). Furthermore, plasmablast differentiation is favored over GC development in both the early IgM response and the memory response, wherein B cells with the highest avidity BCR acquire and display the most foreign peptides (50). If peptide density is responsible, it is conceivable that T cell reactivity to prominent clonotypic Ig-derived peptides could play a role in promoting secondary plasmablast responses at the expense of secondary GC development by memory B cells.

The counterargument against peptide density is that affinity-enhancing somatic mutations promote memory B cell development, and B cells with receptors of highest affinity should present the most antigenic peptide in MHC II to T_{FH} cells (1, 51). Thus, one might expect that if a high level of peptide presentation in MHC II inhibited GC B cells, affinity maturation in memory B cells would be impaired. In addition, CD4 T cells expressing receptors of highest affinity for peptide/MHC II seem to be favored for recruitment into the T_{FH} compartment, with full differentiation requiring secondary cognate T–B interactions (52, 53). Unfortunately, determining the level of BCR-derived peptide versus Ag-derived peptide displayed within MHC II among GC B cells in our model is technically prohibitive.

An alternative to peptide–MHC II density as a determinant of B cell development is the possibility that the kinetics of peptide presentation by GC B cells determines their fate. Affinity maturation in memory B cells to conventional exogenous Ag may require temporally regulated peptide display in MHC II by B cells as they seek T cell help in a functional test for beneficial somatic mutations. Periods of peptide display in MHC II,

punctuated by intervals of MHC turnover without peptide display, would provide a mechanism for sequentially testing somatic mutations as they are acquired stepwise during the GC reaction. B cell migration between the dark and light zones of the GC could be a physical manifestation of such a process. BCR-derived peptides, in contrast, may be continuously displayed in B cell MHC II, even when the BCR is not engaged with Ag. This is plausible because κTg B cells that are activated by LPS without BCR cross-linking proficiently display the VκFR1 peptide in I-A^k (16). According to this scenario, termination of memory B cell development and differentiation into short-lived extrafollicular plasmablasts would either be due to B cell stimulation by conventional T_{FH} cells at inappropriate times or due to a qualitatively unique form of stimulation by a novel subset of T follicular cells that have acquired an altered regulatory phenotype in response to continuous interactions with GC B cells or processed Ig. Determining whether GC disruption by BCR peptide-specific T cells is due to peptide presentation kinetics, density in MHC II, or unique T cell phenotypic characteristics will require further investigation and perhaps a modification of this model that permits comparative analyses of BCR-specific T cells and conventional carrier-specific T cells.

Supplementary Material

Refer to Web version on PubMed Central for supplementary material.

Acknowledgments

We thank Dr. Dennis Huszar for the $\kappa^{-/-}$ mice; Dr. Katja Aviszus, Dr. Thiago Detanico, Dr. Wenzhong Guo, and Greg Kirchenbaum for scientific insights; and Dr. Judith Spiegel for proofreading the manuscript.

This work was supported by National Institutes of Health Grants R01 AI033613 and R01 AI073945 and National Institute of Allergy and Infectious Diseases Grant T32 AI007405.

Abbreviations used in this article

ASC	Ab-secreting cell
CtrlP	control peptide
GC	germinal centers
GαMκ	goat anti-mouse Ig-κ
LN	lymph node
PNA	peanut agglutinin
SHM	somatic hypermutation
T_{FH}	T follicular helper

References

1. Berek C, Griffiths GM, Milstein C. Molecular events during maturation of the immune response to oxazolone. Nature. 1985; 316:412–418. [PubMed: 3927173]
2. Wysocki L, Manser T, Gefter ML. Somatic evolution of variable region structures during an immune response. Proc Natl Acad Sci USA. 1986; 83:1847–1851. [PubMed: 3485290]
3. Tew JG, Wu J, Qin D, Helm S, Burton GF, Szakal AK. Follicular dendritic cells and presentation of antigen and costimulatory signals to B cells. Immunol Rev. 1997; 156:39–52. [PubMed: 9176698]
4. Liu YJ, Joshua DE, Williams GT, Smith CA, Gordon J, MacLennan IC. Mechanism of antigen-driven selection in germinal centres. Nature. 1989; 342:929–931. [PubMed: 2594086]

5. Jacob J, Przylepa J, Miller C, Kelsoe G. In situ studies of the primary immune response to (4-hydroxy-3-nitrophenyl)acetyl. III. The kinetics of V region mutation and selection in germinal center B cells. J Exp Med. 1993; 178:1293–1307. [PubMed: 8376935]
6. Breitfeld D, Ohl L, Kremmer E, Ellwart J, Sallusto F, Lipp M, Förster R. Follicular B helper T cells express CXC chemokine receptor 5, localize to B cell follicles, and support immunoglobulin production. J Exp Med. 2000; 192:1545–1552. [PubMed: 11104797]
7. Chtanova T, Tangye SG, Newton R, Frank N, Hodge MR, Rolph MS, Mackay CR. T follicular helper cells express a distinctive transcriptional profile, reflecting their role as non-Th1/Th2 effector cells that provide help for B cells. J Immunol. 2004; 173:68–78. [PubMed: 15210760]
8. Ansel KM, McHeyzer-Williams LJ, Ngo VN, McHeyzer-Williams MG, Cyster JG. In vivo-activated CD4 T cells upregulate CXC chemokine receptor 5 and reprogram their response to lymphoid chemokines. J Exp Med. 1999; 190:1123–1134. [PubMed: 10523610]
9. Reinhardt RL, Liang HE, Locksley RM. Cytokine-secreting follicular T cells shape the antibody repertoire. Nat Immunol. 2009; 10:385–393. [PubMed: 19252490]
10. Nurieva RI, Chung Y, Hwang D, Yang XO, Kang HS, Ma L, Wang YH, Watowich SS, Jetten AM, Tian Q, Dong C. Generation of T follicular helper cells is mediated by interleukin-21 but independent of T helper 1, 2, or 17 cell lineages. Immunity. 2008; 29:138–149. [PubMed: 18599325]
11. Hande S, Notidis E, Manser T. Bcl-2 obstructs negative selection of autoreactive, hypermutated antibody V regions during memory B cell development. Immunity. 1998; 8:189–198. [PubMed: 9492000]
12. Weiss S, Bogen B. B-lymphoma cells process and present their endogenous immunoglobulin to major histocompatibility complex-restricted T cells. Proc Natl Acad Sci USA. 1989; 86:282–286. [PubMed: 2492101]
13. Weiss S, Bogen B. MHC class II-restricted presentation of intracellular antigen. Cell. 1991; 64:767–776. [PubMed: 1847667]
14. Bartnes K, Hannestad K. Engagement of the B lymphocyte antigen receptor induces presentation of intrinsic immunoglobulin peptides on major histocompatibility complex class II molecules. Eur J Immunol. 1997; 27:1124–1130. [PubMed: 9174601]
15. Munthe LA, Kyte JA, Bogen B. Resting small B cells present endogenous immunoglobulin variable-region determinants to idiotope-specific CD4(+) T cells in vivo. Eur J Immunol. 1999; 29:4043–4052. [PubMed: 10602015]
16. Snyder CM, Zhang X, Wysocki LJ. Negligible class II MHC presentation of B cell receptor-derived peptides by high density resting B cells. J Immunol. 2002; 168:3865–3873. [PubMed: 11937540]
17. Zhang X, Smith DS, Guth AM, Wysocki LJ. A receptor presentation hypothesis for T cell help that recruits autoreactive B cells. J Immunol. 2001; 166:1562–1571. [PubMed: 11160197]
18. Snyder CM, Aviszus K, Heiser RA, Tonkin DR, Guth AM, Wysocki LJ. Activation and tolerance in CD4(+) T cells reactive to an immunoglobulin variable region. J Exp Med. 2004; 200:1–11. [PubMed: 15226360]
19. Munthe LA, Os A, Zangani M, Bogen B. MHC-restricted Ig V region-driven T-B lymphocyte collaboration: B cell receptor ligation facilitates switch to IgG production. J Immunol. 2004; 172:7476–7484. [PubMed: 15187126]
20. Singh RR, Kumar V, Ebling FM, Southwood S, Sette A, Sercarz EE, Hahn BH. T cell determinants from autoantibodies to DNA can up-regulate autoimmunity in murine systemic lupus erythematosus. J Exp Med. 1995; 181:2017–2027. [PubMed: 7539036]
21. Williams WM, Staines NA, Muller S, Isenberg DA. Human T cell responses to autoantibody variable region peptides. Lupus. 1995; 4:464–471. [PubMed: 8749569]
22. Hestvik AL, Vartdal F, Fredriksen AB, Thompson KM, Kvale EO, Skorstad G, Bogen B, Holmoy T. T cells from multiple sclerosis patients recognize multiple epitopes on self-IgG. Scand J Immunol. 2007; 66:393–401. [PubMed: 17850583]
23. Eyerman MC, Zhang X, Wysocki LJ. T cell recognition and tolerance of antibody diversity. J Immunol. 1996; 157:1037–1046. [PubMed: 8757607]

24. Guo W, Smith D, Guth A, Aviszus K, Wysocki LJ. T cell tolerance to germline-encoded antibody sequences in a lupus-prone mouse. J Immunol. 2005; 175:2184–2190. [PubMed: 16081785]
25. Bogen B, Jørgensen T, Hannestad K. T helper cell recognition of idiotopes on lambda 2 light chains of M315 and T952: evidence for dependence on somatic mutations in the third hypervariable region. Eur J Immunol. 1985; 15:278–281. [PubMed: 2579823]
26. Eyerman MC, Wysocki L. T cell recognition of somatically-generated Ab diversity. J Immunol. 1994; 152:1569–1577. [PubMed: 8120370]
27. Clemens A, Rademaekers A, Specht C, Kölsch E. The J558 VH CDR3 region contributes little to antibody avidity; however, it is the recognition element for cognate T cell control of the alpha(1—>3) dextran-specific antibody response. Int Immunol. 1998; 10:1931–1942. [PubMed: 9885915]
28. Chen J, Trounstine M, Kurahara C, Young F, Kuo CC, Xu Y, Loring JF, Alt FW, Huszar D. B cell development in mice that lack one or both immunoglobulin kappa light chain genes. EMBO J. 1993; 12:821–830. [PubMed: 8458340]
29. Lyons AB, Parish CR. Determination of lymphocyte division by flow cytometry. J Immunol Methods. 1994; 171:131–137. [PubMed: 8176234]
30. Marshak-Rothstein A, Siekevitz M, Margolies MN, Mudgett-Hunter M, Gefter ML. Hybridoma proteins expressing the predominant idiotype of the antiazophenylarsonate response of A/J mice. Proc Natl Acad Sci USA. 1980; 77:1120–1124. [PubMed: 6767242]
31. Finkelman FD, Goroff DK, Fultz M, Morris SC, Holmes JM, Mond JJ. Polyclonal activation of the murine immune system by an antibody to IgD. X. Evidence that the precursors of IgG1-secreting cells are newly generated membrane IgD+B cells rather than the B cells that are initially activated by anti-IgD antibody. J Immunol. 1990; 145:3562–3569. [PubMed: 2246501]
32. Fooksman DR, Schwickert TA, Victora GD, Dustin ML, Nussenzweig MC, Skokos D. Development and migration of plasma cells in the mouse lymph node. Immunity. 2010; 33:118–127. [PubMed: 20619695]
33. García De Vinuesa C, Gulbranson-Judge A, Khan M, O'Leary P, Cascalho M, Wabl M, Klaus GG, Owen MJ, MacLennan IC. Dendritic cells associated with plasmablast survival. Eur J Immunol. 1999; 29:3712–3721. [PubMed: 10556827]
34. Hataye J, Moon JJ, Khoruts A, Reilly C, Jenkins MK. Naive and memory CD4+ T cell survival controlled by clonal abundance. Science. 2006; 312:114–116. [PubMed: 16513943]
35. Erickson LD, Durell BG, Vogel LA, O'Connor BP, Cascalho M, Yasui T, Kikutani H, Noelle RJ. Short-circuiting long-lived humoral immunity by the heightened engagement of CD40. J Clin Invest. 2002; 109:613–620. [PubMed: 11877469]
36. Pape KA, Kouskoff V, Nemazee D, Tang HL, Cyster JG, Tze LE, Hippen KL, Behrens TW, Jenkins MK. Visualization of the genesis and fate of isotype-switched B cells during a primary immune response. J Exp Med. 2003; 197:1677–1687. [PubMed: 12796466]
37. Townsend SE, Goodnow CC. Abortive proliferation of rare T cells induced by direct or indirect antigen presentation by rare B cells in vivo. J Exp Med. 1998; 187:1611–1621. [PubMed: 9584139]
38. Moon JJ, Chu HH, Pepper M, McSorley SJ, Jameson SC, Kedl RM, Jenkins MK. Naive CD4(+) T cell frequency varies for different epitopes and predicts repertoire diversity and response magnitude. Immunity. 2007; 27:203–213. [PubMed: 17707129]
39. Pulendran B, Smith KG, Nossal GJ. Soluble antigen can impede affinity maturation and the germinal center reaction but enhance extrafollicular immunoglobulin production. J Immunol. 1995; 155:1141–1150. [PubMed: 7543516]
40. Phan TG, Green JA, Gray EE, Xu Y, Cyster JG. Immune complex relay by subcapsular sinus macrophages and noncognate B cells drives antibody affinity maturation. Nat Immunol. 2009; 10:786–793. [PubMed: 19503106]
41. Aviszus K, Zhang X, Wysocki LJ. Silent development of memory progenitor B cells. J Immunol. 2007; 179:5181–5190. [PubMed: 17911603]
42. Hardtke S, Ohl L, Förster R. Balanced expression of CXCR5 and CCR7 on follicular T helper cells determines their transient positioning to lymph node follicles and is essential for efficient B-cell help. Blood. 2005; 106:1924–1931. [PubMed: 15899919]

43. Smith KG, Light A, Nossal GJ, Tarlinton DM. The extent of affinity maturation differs between the memory and antibody-forming cell compartments in the primary immune response. EMBO J. 1997; 16:2996–3006. [PubMed: 9214617]
44. Bachmann MF, Odermatt B, Hengartner H, Zinkernagel RM. Induction of long-lived germinal centers associated with persisting antigen after viral infection. J Exp Med. 1996; 183:2259–2269. [PubMed: 8642335]
45. Dogan I, Bertocci B, Vilmont V, Delbos F, Mégret J, Storck S, Reynaud CA, Weill JC. Multiple layers of B cell memory with different effector functions. Nat Immunol. 2009; 10:1292–1299. [PubMed: 19855380]
46. Wysocki LJ, Gefter ML, Margolies MN. Parallel evolution of antibody variable regions by somatic processes: consecutive shared somatic alterations in VH genes expressed by independently generated hybridomas apparently acquired by point mutation and selection rather than by gene conversion. J Exp Med. 1990; 172:315–323. [PubMed: 2358780]
47. Allen CD, Okada T, Tang HL, Cyster JG. Imaging of germinal center selection events during affinity maturation. Science. 2007; 315:528–531. [PubMed: 17185562]
48. Okada T, Miller MJ, Parker I, Krummel MF, Neighbors M, Hartley SB, O'Garra A, Cahalan MD, Cyster JG. Antigen-engaged B cells undergo chemotaxis toward the T zone and form motile conjugates with helper T cells. PLoS Biol. 2005; 3:e150. [PubMed: 15857154]
49. Benson MJ, Erickson LD, Gleeson MW, Noelle RJ. Affinity of antigen encounter and other early B-cell signals determine B-cell fate. Curr Opin Immunol. 2007; 19:275–280. [PubMed: 17433651]
50. Paus D, Phan TG, Chan TD, Gardam S, Basten A, Brink R. Antigen recognition strength regulates the choice between extrafollicular plasma cell and germinal center B cell differentiation. J Exp Med. 2006; 203:1081–1091. [PubMed: 16606676]
51. Jacob J, Kelsoe G. In situ studies of the primary immune response to (4-hydroxy-3-nitrophenyl)acetyl. II. A common clonal origin for periarteriolar lymphoid sheath-associated foci and germinal centers. J Exp Med. 1992; 176:679–687. [PubMed: 1512536]
52. Fazilleau N, McHeyzer-Williams LJ, Rosen H, McHeyzer-Williams MG. The function of follicular helper T cells is regulated by the strength of T cell antigen receptor binding. Nat Immunol. 2009; 10:375–384. [PubMed: 19252493]
53. Ebert LM, Horn MP, Lang AB, Moser B. B cells alter the phenotype and function of follicular-homing CXCR5+ T cells. Eur J Immunol. 2004; 34:3562–3571. [PubMed: 15549776]

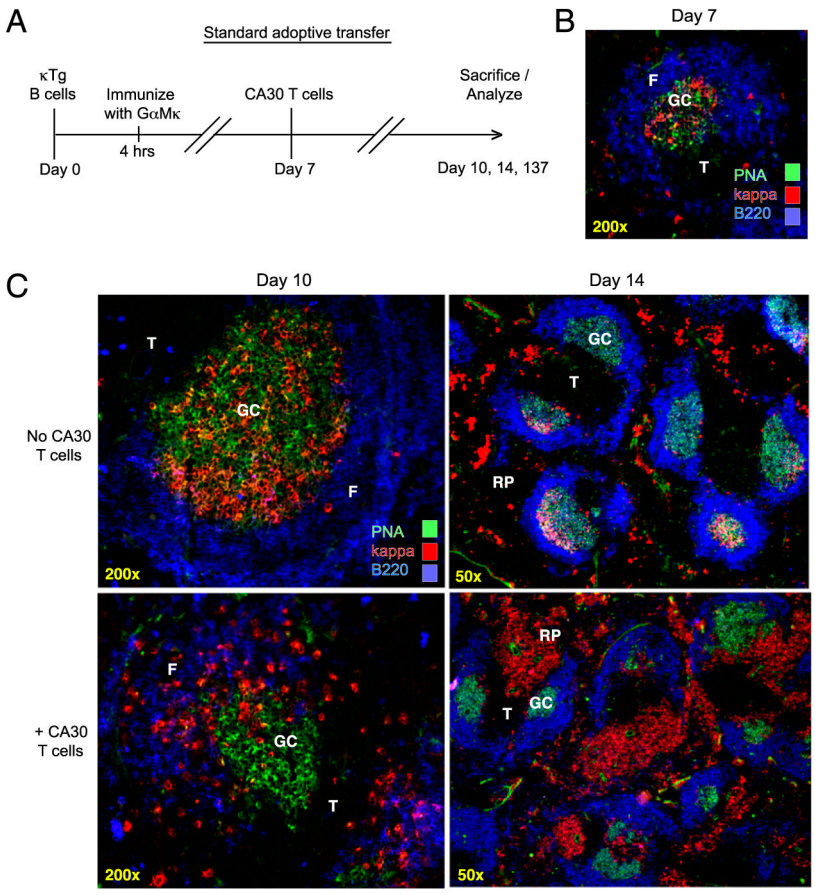

FIGURE 1.

CA30 T cells abort GC responses by κTg B cells. *A*, Standard adoptive transfer: κ L chain-deficient mice ($\kappa^{-/-}$) received 5.0×10^4 $\kappa Tg^{+/-}$ $\kappa^{-/-}$ splenocytes i.v. on day 0. Four hours after transfer, recipients were immunized i.p. with GαMκ precipitated in alum. On day 7, the experimental group received 2.5×10^5 LN cells i.v. from CA30 $\kappa^{-/-}$ donors. Groups of recipients were sacrificed on days indicated. *B*, Representative image of day 7 GC. Sections stained with PNA and mAb directed to indicated Ags. *C*, Representative images of individual day 10 splenic GC (*left*), and of day 14 spleen (*right*) in mice that received (*bottom*) or did not receive (*top*) CA30 T cells at day 7. Images are representative of at least five independent experiments with between three and five mice per group. See also Supplemental Fig. 1. F, B cell follicle; RP, red pulp; T, T cell zone.

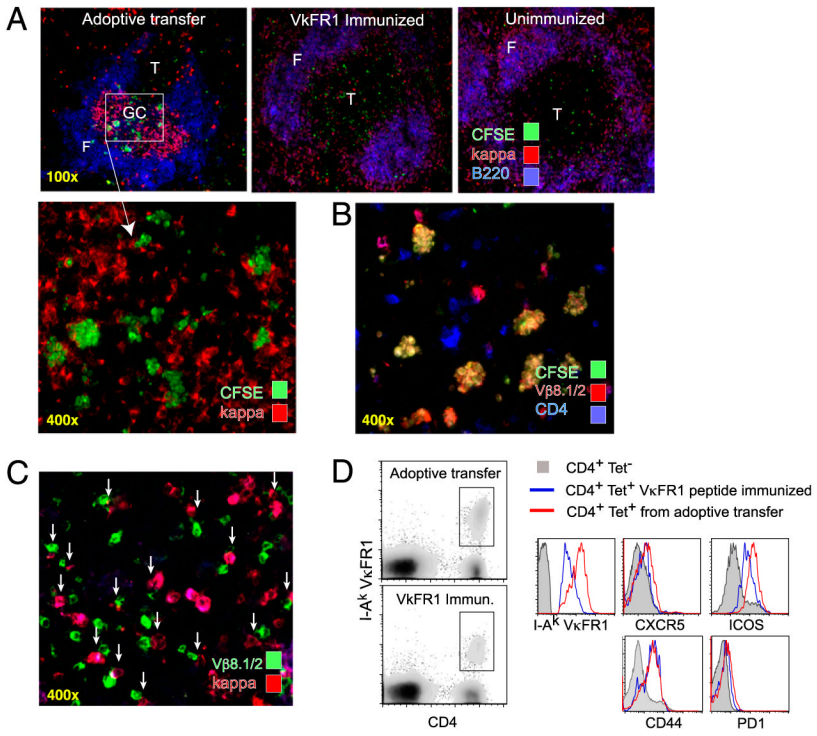

FIGURE 2.

Rapid activation and migration of CA30 T cells to GC containing κTg B cells. *A*, Representative images of spleens from adoptive recipients of κTg cells (*left*), control VκFR1 peptide-immunized mice (*center*), or control unimmunized mice (*right*) that received enriched CFSE-labeled CA30 T cells (>90%) 50 h earlier. A/J recipient mice were used for VκFR1 peptide-immunization and no-immunization groups. Experimental group (*top left*) received CA30 T cells at day 7 following transfer of κTg splenocytes and immunization with GαMκ (alum). VκFR1 peptide immunization (alum) occurred at the time of CA30 transfer. CFSE staining of CA30 T cells was amplified with an Alexa-488–labeled anti-FITC mAb. *B*, $CFSE^+$ cells in GC of mice that received κTg cells costain with both anti-CD4 and anti-Vβ8.1/2, as listed. *C*, Representative image of day 14 splenic GC from adoptive transfer recipients. Arrows highlight cognate interactions between $κ^+$ B cells and Vβ8.1/8.2 T cells. *D*, Comparative expression levels of CXCR5, ICOS, CD44, and PD-1 among $CD4^+$ $I\text{-}A^k$-$VκFR1^+$ T cells 3 d after transfer of CA30 T cells. Experimental mice (red) received κTg B cells and were immunized with GαMκ (alum) 7 d before CA30 transfer. Control mice (blue) received CA30 T cells and were immunized with VκFR1 peptide in alum 3 d previously. Filled histogram represents $CD4^+$ VκFR1 tetramer-negative T cells from experimental group. Results are representative of at least three independent experiments with three to five mice per group.

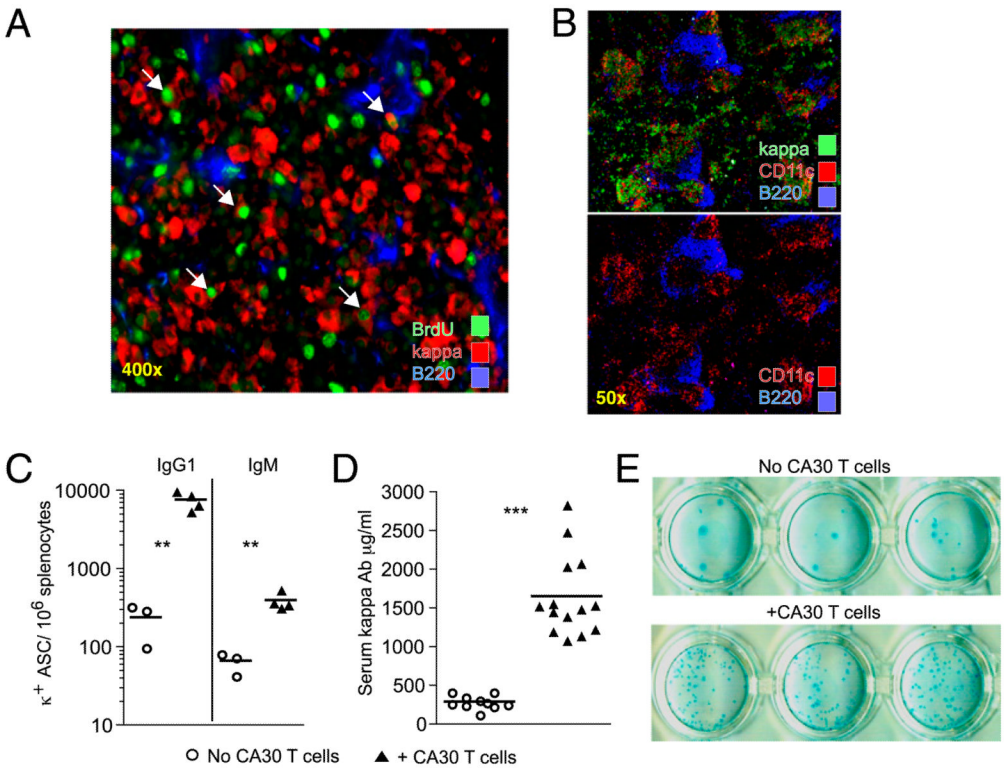

FIGURE 3.

Plasmablast phenotype of κTg cells 7 d following transfer of CA30 T cells. *A*, Day 14 image of κTg B cells clustered in the splenic red pulp of a recipient of CA30 $\kappa^{-/-}$ T cells. Arrows highlight κ^+ cells (red) with $BrdU^+$ nuclei (green). Images are representative of two independent experiments. *B*, Duplicate images of a representative day 14 spleen from a mouse that received κTg cells on day 0 and CA30 T cells on day 7. *Bottom image* shows CD11c staining in the absence of anti-κ fluorescence. Images are representative of three independent experiments. *C*, Frequency of day 14 κ^+ $IgG1^+$ and κ^+ IgM^+ splenic ASC determined by ELISPOT. Data are representative of at least three independent experiments with three to five mice per group. *D*, Serum κ^+ Ab concentration at day 14. Three independent experiments are represented in this plot. *C* and *D*, Symbols represent individual mice, with lines representing mean values. Statistically significant differences are indicated (**$p \leq 0.01$, ***$p \leq 0.001$, as determined by a two-tailed *t* test). *E*, Representative $IgG1^+$ κ^+ ELISPOT from day 14 spleens of mice that received κTg cells and CA30 $\kappa^{-/-}$ T cells (*bottom*) or not (*top*). ELISPOT images are representative of at least three independent experiments with three to five mice per group.

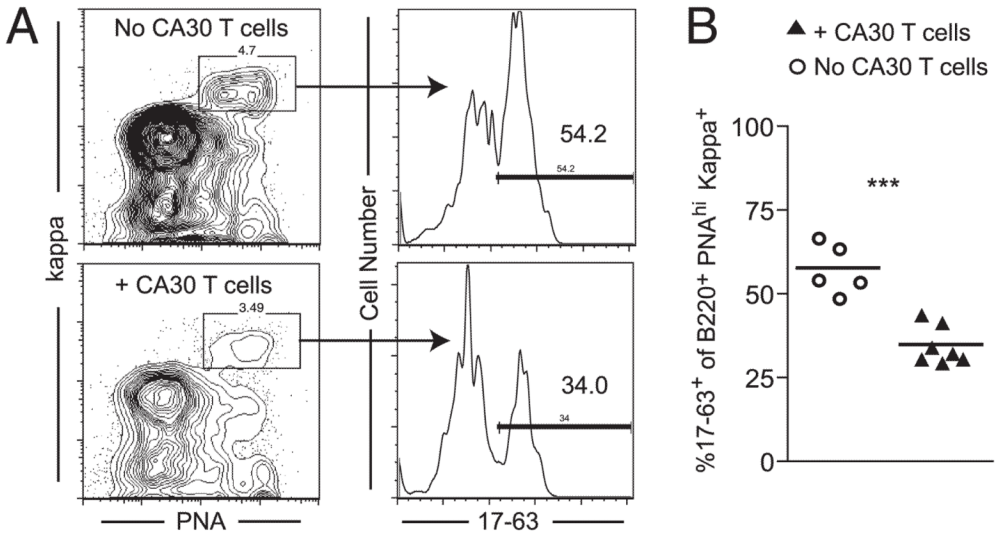

FIGURE 4.

CA30 T cells selectively inhibit development of κTg B cells in GC. *A*, Flow cytometric plot showing the gating strategy for the analysis of the proportion of κTg B cells, among all κ^+ B cells, within GC or recipient mice. Mice received a 1:1 mixture of purified κTg $\kappa^{-/-}$ and A/J B cells on day 0. CA30 $\kappa^{-/-}$cells were transferred to the experimental group on day 7. On day 10, $B220^+$ splenocytes were gated for κ^+ PNA^{high} cells, and the percentage of these staining with mAb17-63 was determined. *B*, Quantification of the percentage of $17\text{-}63^+$ (κTg) B cells, among all κ^+ cells, within the $B220^+$ PNA^{high} gate, as described in *A*. Symbols represent individual mice pooled from two independent experiments, with lines representing mean values. Statistically significant differences are indicated. See also Supplemental Fig. 2. $^{***}p \leq 0.001$ as determined by a two-tailed *t* test.

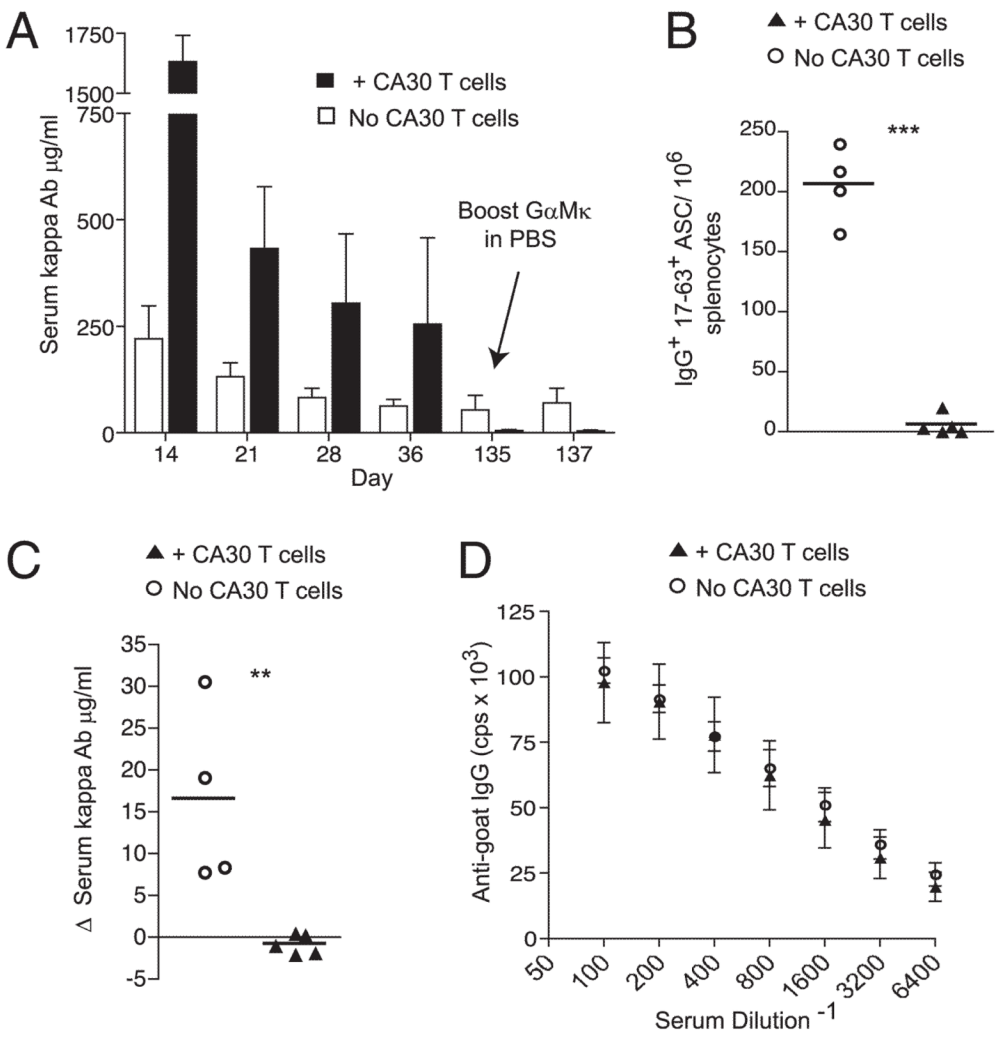

FIGURE 5.

Inhibition of a κTg memory response by CA30 T cells. *A*, Time course of serum κ^+ Ab in mice that received ($n = 5$, ■) or did not receive ($n = 4$, □) CA30 $\kappa^{-/-}$ T cells on day 7. *Tops* of bars represent mean values for the group, with SEM shown. Note virtual absence of κ^+ Ab in CA30 recipients at day 135 despite high titers on day 14. Data are representative of three independent experiments with three to five mice per group. *B*, Frequency of $IgG1^+$ $17\text{-}63^+$ splenic ASC 50 h following boost. *C*, Change in serum κ^+ Ab concentration 50 h following booster injection on day 135. *B* and *C*, Symbols represent individual mice, with lines representing mean values. Data are representative of three independent experiments with three to five mice per group. Statistically significant differences are indicated. $^{**}p \leq 0.01$, $^{***}p \leq 0.001$ as determined by a two-tailed *t* test. *D*, Serum IgG^+ Ab titers against goat IgG at 50 h after boost. Symbols represent mean values for each group ($n = 5$; +CA30 T cells; $n = 4$, No CA30 T cells) with SEM shown. Data are representative of three independent experiments.

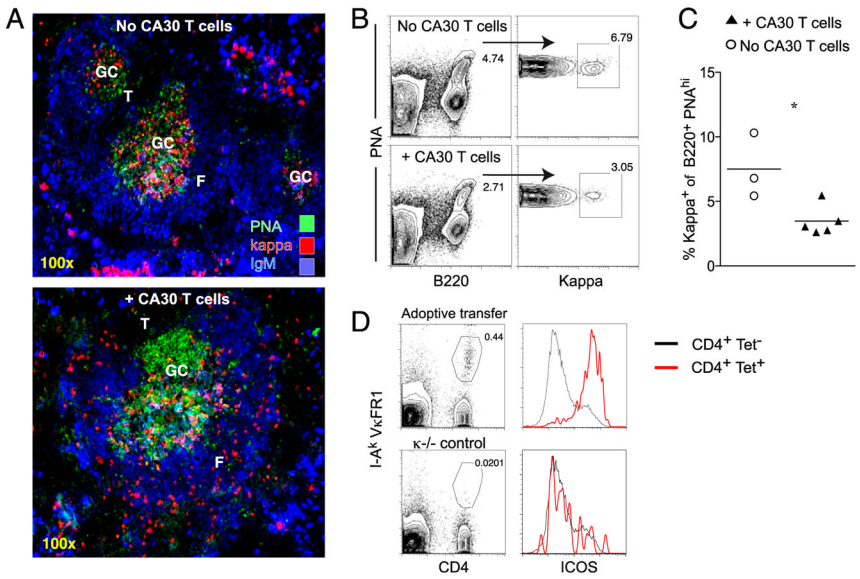

FIGURE 6.

GC development inhibited in recipients of small numbers of transferred cells. All mice received 5.0×10^3 κTg splenocytes on day 0, followed by immunization with GαMκ in alum i.p. Mice in the experimental group received 5.0×10^3 CA30 LN cells on day 6. Recipient spleens were collected on day 12. *A*, Representative images of day 12 splenic GC in experimental and control mice. *B*, Representative flow cytometric gating strategy of day 12 spleens for GC occupancy by κ^+ cells. The percentage of κ^+ cells among total $B220^+$ PNA^{high} splenocytes was determined. *C*, Quantification of the percentage of GC occupied by κ^+ B cells on day 12 in mice that received (▲) or did not receive (○) CA30 LN cells, as described above. Symbols represent individual mice, with lines representing mean values. Statistically significant differences are indicated (*$p \leq 0.05$, as determined by a two-tailed *t* test). *D*, Representative day 12 tetramer staining and ICOS expression of splenocytes in recipients of 5.0×10^3 CA30 LN cells on day 6. Data in *A*–*D* are representative of two independent experiments with three to five mice per group.

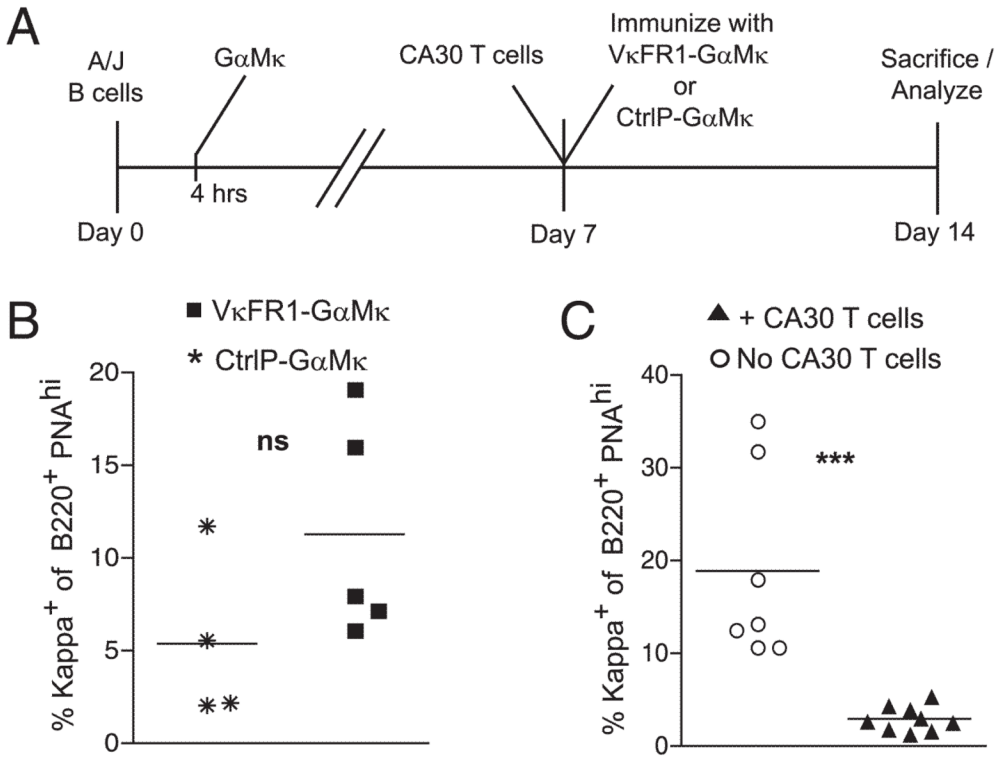

FIGURE 7.

CA30 T cells do not impair the GC response by B cells that exogenously acquire the VκFR1 peptide. *A*, Adoptive transfer scheme designed to provide CA30 T cell help to A/J B cells presenting exogenously derived VκFR1 peptide. $\kappa^{-/-}$ mice received 5.0×10^4 A/J splenocytes on day 0. Four hours after transfer, recipients were immunized i.p. with 50 μg GαMκ precipitated in alum. On day 7, both groups received 2.5×10^5 CA30 $\kappa^{-/-}$ LN cells, followed by i.p. immunization with either VκFR1-GαMκ or CtrlP-GαMκ in alum. Mice were sacrificed on day 14. *B*, Percentage of total $B220^+$ PNA^{high} (GC) splenocytes that were κ^+ on day 14 in mice immunized with VκFR1-GαMκ (■) or CtrlP-GαMκ (*) on day 7. Data are representative of two independent experiments with four to five mice per group. *C*, Percentage of total $B220^+$ PNA^{high} (GC) splenocytes that were κ^+ on day 14 following transfer of κTg splenocytes (day 0), followed by day 7 CA30 transfer (▲), compared with no CA30 transfer (○), the standard adoptive transfer protocol described in Fig. 1*A*. Results represent data from two independent experiments with three to five mice per group. Symbols in both *B* and *C* represent individual mice, with lines representing mean values. Statistical differences are indicated. See also Supplemental Fig. 4. ***$p \leq 0.001$, as determined by a two-tailed *t* test. ns, not significant.